ALGORITHM FOR MANUFACTURING ACCURATE AL-SI ALLOY CAST PARTS

Florin Susac, Nicuşor Baroiu

"Dunărea de Jos" University of Galați, Department of Manufacturing Engineering,
Domnească Street, No. 111, 800201, Galați, România

Corresponding author: Nicuşor Baroiu, nicusor.baroiu@ugal.ro

Abstract: Cast parts manufacturing has some disadvantages as dimensional accuracy of the parts which is generally lower if comparing with parts manufactured by other processes. This paper presents an algorithm for manufacturing very accurate cast parts made of Al-Si alloys, based on FEM analysis and artificial neural network (ANN). The paper also presents an analytical technique for estimating the dimension of air gap formation at the cast/mold interface during solidification and cooling of melt alloy. As the final dimension of the cast part is directly determined by air gap evolution, short explanation about this phenomenon is given.

Key words: algorithm, ANN, casting, dimensional accuracy, shrinkage.

1. INTRODUCTION

An essential condition for manufacturing quality products is to respect the geometrical (linear and angular) parameters of the parts. To obtain the dimensions which define the part geometry at their nominal value (theoretical value) is not possible because of the manufacturing and measurement errors. The manufacturing techniques allow the obtaining of the final dimension of the part with an approximate precision if compare with nominal dimension (prescribed dimension). Also, the measurement methods do not allow a very accurate measurement of the part dimensions due to specific errors of measurement instruments, errors of measuring and reading the instruments indications and surfaces relief, or due to other factors.

Therefore, we can distinguish (i) cast part macro-geometry accuracy, which refers to dimensional precision, geometry precision, precision of geometric elements position and (ii) cast part micro-geometry precision, which mainly refers to surface roughness.

When casting, all surfaces of the part are simultaneously generated, which is different then machining processes when only one surface is generated at the time.

Epureanu et al. [1] stated that, in casting, there is no reference surface; the only reference is mold surface, which is considered as programmed surface. The cast part surface is considered as realized (manufactured) surface. The difference between the two surfaces is manufacturing error.

Dimensionally, the casting process consists in manufacturing a part whose dimensions are according to the limits mentioned in design drawing of the product. Considering the idea of dimensionally controlling the casting process, it is considered that casting has three stages: a) prognosis; b) programming and c) casting.

In the last years, many simulation tools of the casting process have been developed, but these software does not offer a very accurate simulation of the real casting process.

After is poured in the mold, the melt takes its shape during solidification and cooling. After melt reaches liquidus temperature, the transition from liquid state to solid state begins. The solidification rate is determined by the rapidity of removing heat and characterizes the growth of the solid state with respect to time. For the majority of the metals, the transition between the two phases determines volume shrinkage. For aluminum alloys, the volume shrinkage due to solidification is between 3.5…8.5%, Kaufman and Rooy [2].

There are a few studies concerning the permanent mold casting process control, most of the research focuses on continuous casting. In this direction, important work is made by Bouhouche et al. [3], Fitzgerald et al. [4], Guo et al. [5], Ikeda et al. [6], Kuzminov et al. [7], Kong et al. [8], Lotov et al. [9] and Maijer et al. [10].

An essential research direction is the study of heat transfer coefficient at the cast/mold interface. The importance of estimating heat transfer coefficient is obviously considering that thermal field dynamics during solidification is a major factor which influences the cast part dimensional accuracy and surface quality.

Relevant work was carried out by Zhang et al. [11]. They studied the interfacial heat transfer coefficient by developing an inverse heat transfer analysis

procedure based on least squares technique and sequential function specification method.
Moreover, Xu et al. [12] focused on the study of peak value of heat transfer coefficient at the cast mold interface. They concluded that the new method improves the prediction accuracy. Their method, based on Hamasaiid model, can be used to simplify the surface profile in the improved model.
Relevant study concerning the air gap formation mechanism at the cast mold interface and the heat transfer through the gap was made by Nishida et al. [13]. The displacement of the inner wall of the mold δm is given by:

$$\delta_m = \frac{2R_i \cdot \alpha\left(1+\upsilon\right)}{R_e^2 - R_i^2}\int_a^b T\left(r,t\right) rdr \qquad (1)$$

where: R_i is inner radius of the mold [mm], R_e is the outer radius of the mold [mm], α is linear thermal expansion coefficient of the mould [K^{-1}], υ is Poisson ratio and $T(r,t)$ is radius and time dependent temperature [°C].
Although between continuous casting and permanent mold casting many differences exist, there are some similarities concerning the main objective which refers to the modality of extracting heat from cast part without affecting the dimensional accuracy of the part.
Susac [14] states that, in permanent mold casting, the designing and manufacturing stages can be integrated in order to obtain a better correlation between the mechanical properties and the stresses state during part functionality and a better dimensional precision of the part, which is mainly affected by solidification shrinkage.
Dimensionally, the goal of any technological process is to manufacture parts with dimensions that are within the allowance limits mentioned on the design drawing. This means that the part surface must belong to an infinity of admissible surfaces, which is defined by the allowance's limits of this surface, after Epureanu [15].

2. THE DESIGN OF EXPERIMENT

The scheme of the casting set-up, Figure 1, and details concerning the temperature and displacement monitoring were presented by Susac [16]. A hollow cylinder part was cast inside a mold with outer wall and inner core both made of steel. While the mold is bottom insulated, the core is cooled by water at room temperature in order to create a temperature gradient mainly on radial direction.
During the alloy solidification and cooling, the temperature on radial direction and cast displacement were monitored by K-type thermocouples and linear variation displacement transducers and recorded.
The experimental set-up consists in two main modules: casting and parameters measurement module and experimental data acquisition module. The experimental data acquisition module contains a module of analogical inputs for connecting with thermocouples and o module for connecting with displacement transducers.

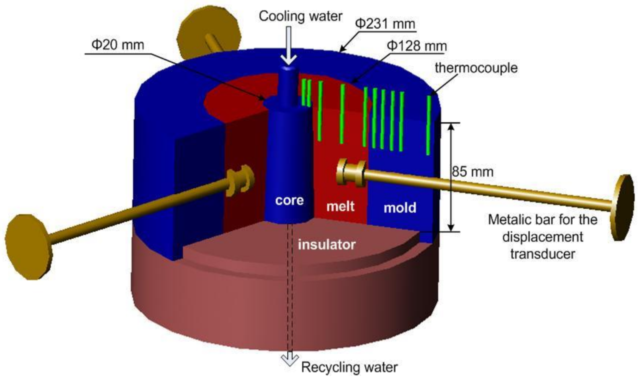

Fig. 1. Casting module of the experimental set-up, after Susac [14]

Susac et al. [17] explained that the air gap formation at the cast/mold interface occurs when the solid shell becomes strong enough to withstand the metalo-static pressure and, therefore, departs from the mold wall due to shrinkage. The air gap formation dramatically reduces the heat transfer through the cast/mold interface and therefore the solidification is affected.
Lagerstedt [18] founds that, Before the air gap occurs, the heat transfer is mainly by conduction. When the air gap is formed, the heat transfer is reduced and may be described as a combination between radiation and conduction. For aluminum, the heat transfer by radiation is insignificant and can be neglected. The heat transfer by convection can be also neglected because the air gap has a small thickness. The general explanation on the air gap formation is the thermal shrinkage of the solid shell that occurs due to temperature drop at the surface and due to resulting temperature gradients, after Susac et al. [17].
The numerical model used for simulation was axisymmetric. Therefore, only a ten degrees portion of the part was used for numerical simulation. This determined a reduction of the simulation time until approximately 4 minutes. The mold and part geometry were meshed into hexahedron finite elements with 8 nodes.

3. ALGORITHM FOR MODELING AND SIMULATION OF THE CASTING PROCESS

The algorithm for modeling and simulation of the casting process of a hollow cylinder cast part is show in Figure 2. This algorithm aims to optimize the casting process in order to obtain dimensional precision, which is imposed by manufacturing standards.
The algorithm for modeling and simulation includes 3 modules:

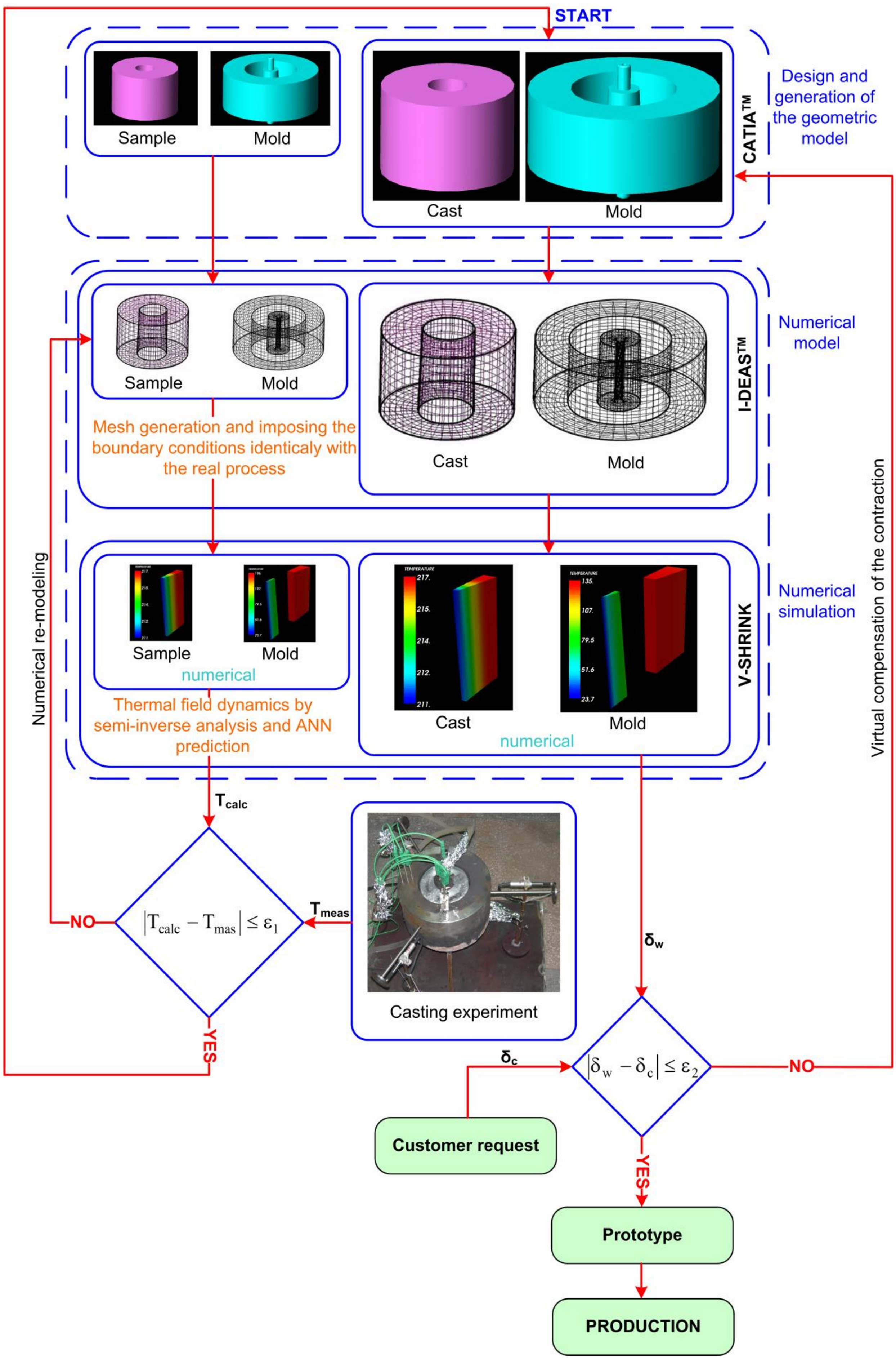

Fig. 2. Algorithm for modeling and simulation of the casting process of a hollow cylinder cast part

a) Module 1 consists in designing and generating the geometric model of the cast part and mold; b) Module 2 consists in generating the numerical model of the casting process; c) Module 3 consists in numerical simulation of the casting process using finite element method.

At the beginning, a geometric model is designed and generated, consisting in one sample and its mold. After generating the mesh of the geometric model, the thermal and mechanical boundary conditions are imposed to the cast, identically with the real process. The thermal field dynamics in different locations of the sample and mold is calculated using an algorithm of semi-inverse analysis, which calls for external software V-Shrink. Simultaneously, using the same algorithm of semi-inverse analysis the evolution of heat transfer coefficient at the cast/mold and cast/core interfaces is determined.

At the same time, the real casting process of the sample is carried-out and the measured thermal field dynamics (in the same locations where is calculated by semi-inverse method) is compared with the calculated thermal field dynamics. If the difference between the measured (T_{mas}) and calculated (T_{calc}) values of the thermal field dynamics is over a maximum value (T_{calc}-$T_{mas} > \varepsilon_1$, where $\varepsilon_1 = 5\%$), then the casting process of the sample will be remodeled (the dimensions of the finite elements will be smaller, the boundary conditions will be revised etc.). If this difference is no more than 5% (T_{calc}-$T_{mas} \leq \varepsilon_1$), the geometric model of an industrial part and its mold will be designed and generated. Using the same procedure, the mesh of the geometric model will be generated and boundary conditions will be imposed as in real process. The solidification/cooling process may be simulated using a finite element software, as V-Shrink.

Finally, if the difference between the final value of the calculated contraction δ_w, see equation (2), and the final value of the measured contraction δ_c (customer requested), is over the imposed value ε_2 (δ_w - $\delta_c < \varepsilon_2$, where $\varepsilon_2 = 10\%$), the mold dimension will be compensated and the previous steps will be completed again.

The programmed path of the thermal field is based on temperature-time-transformation diagram (TTT diagram) of the cast alloy. The cast part will have the imposed dimensions if the thermal field dynamics is identical to the programmed one, i.e. the heat transfer evolution at the cast/mold interface, obtained by numerical simulation, will be identical to the evolution obtained from experimental data, in any location of the cast.

When the customer requests that the cooling curve should cross the transformation lines following a specified path, some parameters (cooling water temperature, mold temperature) will be modified and the thermal field dynamics will be calculated for the desired location. Depending on the calculation result, the same parameter or other parameter will be modified, and the thermal filed dynamics will be calculated again. This will be repeated until the result is the programmed one. Thus, the dimensional precision of the cast part will be controlled.

Based on the numerical results obtained by using the algorithm in Figure 2, it will be decided whether the cast has reached the qualitative and dimensional requirements.

If these desiderates are not reached, virtual compensation will be applied to the mold and the algorithm will be run again. If these desiderates are reached, the next step will be the manufacturing of the prototype followed by the manufacturing of the entire batch of the parts.

3.1 The calculation of the dimension of air gap which forms at the cast/mold interface

After the mold filling is completed, the mold wall moves on radial direction (expansion) because of the high temperature of the melt and the solidified portion of the cast shrinks during cooling.

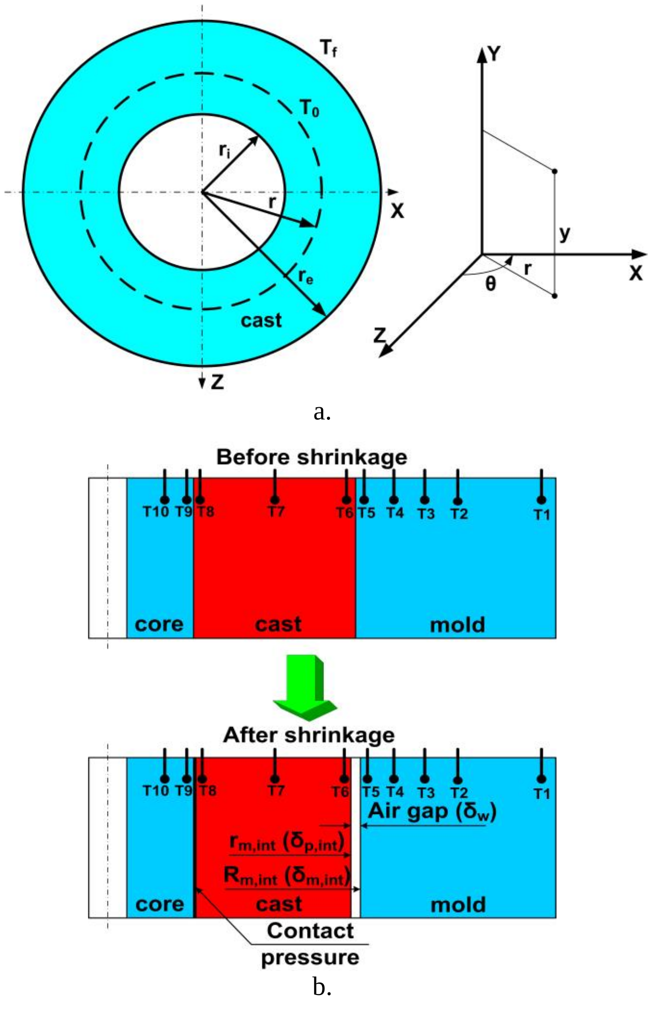

Fig. 3 - a. Scheme of the geometric model used for deformation calculation; b. Air gap formation mechanism

Therefore, the relative movements of both surfaces form an air gap. It is considered that the difference between both displacements (measured and/or calculated) determines the air gap dimension.

$$\delta_w = \delta_m - \delta_p, \quad (2)$$

where δ_w is the dimension of the air gap which forms at the cast/core interface [mm], δ_m is the displacement of the mold wall [mm] and δ_p is the displacement of the cast wall [mm].
The scheme of the simplified geometric model used for thermal deformation calculation and the air gap formation mechanism are shown in Figure 3.

3.2 The displacement of the inner wall of the mold

The displacement of the outer wall of the cast was directly measured by displacement transducers. Therefore, the displacement of the inner wall of the mold was calculated, using equation (3):

$$\delta_{m,\text{int}} = \alpha \cdot r_{m,\text{int}} \cdot \Delta T, \quad (3)$$

where $\delta_{m,int}$ is the displacement of the inner wall of the mold [mm], $r_{m,int}$ is outer radius of the cast [mm] and ΔT – temperature variation within a time increment [K].
The displacement of the inner wall of the mold is calculated for each time increment using the following equation [17]:

$$\dot{\delta}_{m,\text{int}}(t) = r_{m,\text{int}} \cdot \alpha \cdot \left(T(t)\right) \cdot d\dot{T}, \quad (4)$$

where T is mold temperature [°C] and t is time [s].
By integer and if $\alpha = \alpha_{med}$, the following equation is obtained:

$$\delta_{m,\text{int}}(T) = r_{m,\text{int}} \cdot \alpha_{med}\left(T - T_0\right), \quad (5)$$

where $r_{m,int}$ is the inner radius of the mold [mm] and (T-T_0) is the variation of mold temperature within a time increment [°C].
If it is considered that the evolution of the linear expansion coefficient depends on the temperature, i.e.:

$$\alpha(T) = \alpha_0 + k\left(T - T_0\right), \quad (6)$$

where k is a constant and α_0 is linear expansion coefficient at temperature T_0. Therefore:

$$\delta_{m,\text{int}} = \int_{T_0}^{T} \left[\alpha_0 + k\left(T - T_0\right)\right] \cdot dT \quad (7)$$

And, by developing and solving equation (7), the following relation is obtained:

$$\delta_{m,\text{int}} = \alpha_0\left(T - T_0\right) + \frac{k\left(T - T_0\right)^2}{2}. \quad (8)$$

3.3 The calculation of the thermal deformations

Radial deformation (on x axis direction), longitudinal deformation (on y axis direction) and angular deformation are given by the following equations:

$$\varepsilon_\theta = \alpha\left(T_f - T_0\right); \quad \varepsilon_y = \alpha\left(T_f - T_0\right); \quad \varepsilon_r = \alpha\left(T_f - T_0\right), \quad (9)$$

where ε_θ is angular deformation (with θ – variable parameter), ε_y is longitudinal deformation, ε_r is radial deformation, T_f is cast temperature after deformation [°C] and T_0 is cast temperature before deformation [°C].
By imposing the boundary conditions (10):

$$\begin{cases} u_\theta = 0 \\ u_y \neq 0 \\ u_r \neq 0, \end{cases} \quad (10)$$

where: u_θ, u_y, u_r are the displacements on angular, longitudinal and radial directions [mm], equations (11) are obtained:

$$\varepsilon_\theta = \frac{u_r}{r}, \quad \frac{u_r}{r} = \alpha\left(T_f - T_0\right); \quad \varepsilon_y = \frac{\partial u_y}{\partial y}, \quad \frac{\partial u_y}{\partial y} = \alpha\left(T_f - T_0\right); \quad \varepsilon_r = \frac{\partial u_r}{\partial r}, \quad \frac{\partial u_r}{\partial r} = \alpha\left(T_f - T_0\right). \quad (11)$$

where r is a certain radius of the cast [mm], see Figure 3.
Equalizing equations (10) and (11), it results:

$$u_\theta = \alpha \cdot r\left(T_f - T_0\right); \quad u_y = \alpha \cdot y\left(T_f - T_0\right) + C_1; \quad u_r = \alpha \cdot r\left(T_f - T_0\right) + C_2, \quad (12)$$

where C_1 and C_2 are two constants.
If $y = 0$ and $u_y = 0$, then $C_1 = 0$, where y is the cast part (cylinder) height [mm].
While the displacement on longitudinal and angular directions in casting are not important and therefore can be neglected, the radial displacement is determined:

$$u_r(r_i) = \alpha \cdot r_i (T_f - T_0);$$
$$u_r(r_e) = \alpha \cdot r_e (T_f - T_0). \quad (13)$$

where r_i, r_e are the inner radius of the mould, respectively the outer radius of the cast [mm].

3.4 The artificial neural network model

In order to control the path of the thermal field dynamics in the cast an artificial neural network was used. The neural model scheme is presented in Figure 4.

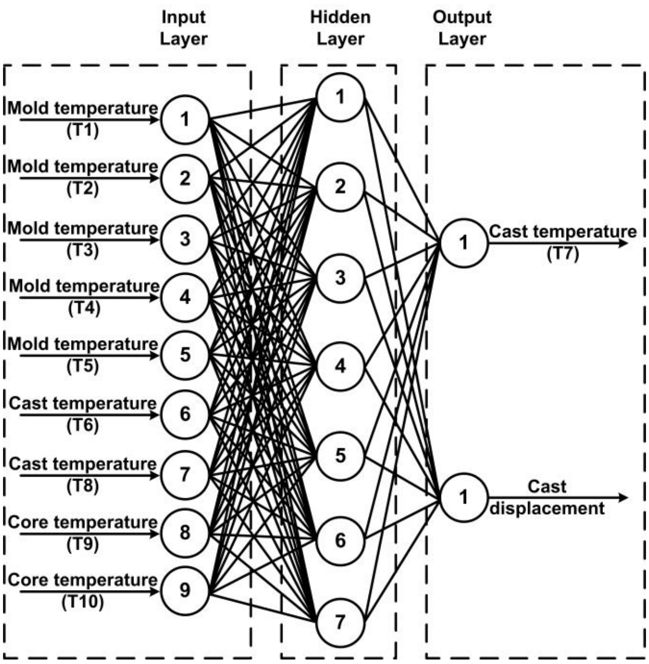

Fig. 4. The scheme of the artificial neural network model

The neural network has 3 layers: the input layer (9 neurons), the hidden layer (7 neurons) and the output layer (2 neurons). The two neurons on the output layer are the temperature in a certain location of the cast, specified by the customer and the cast displacement.

It was found by the best model search function that thermocouples T5 and T9, see Figure 3b, has the greatest influence on thermal field dynamics path in the cast part. The neural model was created based on experimental results.

Thermal field dynamics path during solidification/cooling can be controlled by modifying the temperature in the mold and core. This can be made by modifying the cooling water rate or water temperature. Moreover, additional cooling channels can be designed in the mold. The manner the cast temperature is controlled strongly depends on how the thermal field dynamics should evoluate (according to customer request).

4. RESULTS AND DISCUSSION

The numerical and the experimental results presented in this paper are the starting point to conceive and test a scheme to control the casting process in permanent metallic mold. This control scheme is based on both the thermal field dynamics monitoring of the casting system components and thermal field dynamics prediction of the cast part.

The formation and evolution of air gap at the cast/mold interface affects the heat transfer through the interface and has a direct influence on cast part precision.

The numerical validation of the algorithm is presented in Figures 5 and 6.

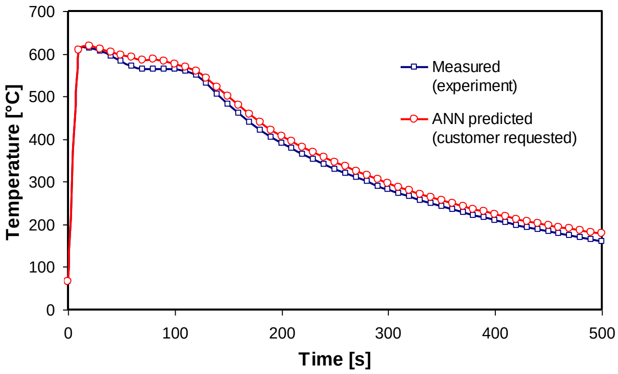

Fig. 5. Experimental and customer requested time dependant temperature of the cast

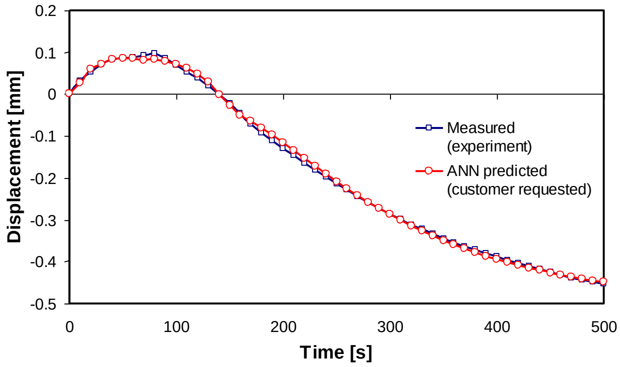

Fig. 6. Experimental and predicted displacement of the cast part

Figure 5 presents the thermal field dynamics of the cast in a certain location indicated by the customer. In order to improve the mechanical properties of the cast such as strength, the customer designed a solidification/cooling path. This path should be followed during casting solidification/cooling, according to the algortihm presented in Figure 2, in order to manufacture accurate parts. Figure 6 presents the displacement of the outer wall of the cast during solidification/cooling. These data will be later used to calculate de air gap dimension which occurs at the cast/mold interface during melt solidification, see equation 2 and Figure 3a.

There is a good agreement between experimental and predicted data, the average error in case of temperature is 4.96% and the average error in case of displacement is 7.25%. The error between experimental and predicted displacement is very low considering that this parameter has very low values as tenths of milimeters.
The algorithm presented in this paper aims the optimization of the casting process related to dimensional precision and mechanical properties of the cast parts according to imposed manufacturing standards or client request. The algorithm architecture offers a systematic approach of numerical simulation techniques.
By using this algorithm, the designing and manufacturing stages can be integrated in a virtual environment that allows the run of all steps starting from CAD geometry generation and finishing with the dimensional precision requested by client.

5. CONCLUSIONS

An algorithm for modeling and simulation of the casting process of a hollow cylinder cast part was presented. The algorithm aims to optimize the casting process in order to obtain dimensional precision, which is imposed by manufacturing standards or customer request.
Based on experimental results an artificial neural network model was generated in order to control the path of the thermal field dynamics.
The error between the measured and predicted thermal field dynamics is 4.96 % and the error between the measured and predicted displacement is 7.25%.
The results are in very good agreement and validate the presented algorithm. This algorithm may be used in foundry if a proper neural control scheme of the casting process is designed and set up.

6. ACKNOWLEDGEMENTS

This work was supported by a grant of the Romanian National Authority for Scientific Research and Innovation, CNCS – UEFISCDI, project number PN-II-RU-TE-2014-4-0031.

7. REFERENCES

1. Epureanu, A., Susac, F., Constantin, I., Buruiană, F., Banu, M, (2007). The Annals of "Dunărea de Jos" University of Galati, Fascile V, 141-144.
2. Kaufman, J. G., Rooy, E.L., (2004). ASM International, 49.
3. Bouhouche, S., Lahreche, M., Bast, J., (2008). Acta Automatica Sinica, 34, 701-706.
4. Fitzgerald, T. J., Singer, R., F, (1997). Met. Mat. Trans. A, 28(6), 1377-1383.
5. Guo, L., Tian, Y., Yao, M., Shen, H., (2009). Int. J. Min. Met. Mat., 6(6), 626-631.
6. Ikeda, T., Ravi, V. A., Snyder, G. J., (2009). Met. Mat. Trans. A, 41(3), 641-650.
7. Kuzminov, A. L., Golubev, A. V., Kozhevnikov, A. V., Shchegolev, N., A., (2009). Metallurgist, 53(3-4), 209-214.
8. Kong, L.X., She, F.H, Gao, W.M, Nahavandi, S., Hodgson, P.D., (2008). J. Mat. Proc. Tech., 629-634.
9. Lotov, A.V., Kamenev, G. K., Berezkin, V.E., Miettinem, K., (2005). Applied Mathematical Modelling, 653-672.
10. Maijer, D.M., Owen, W. S., Vetter, R. A., (2009). Journal of Materials Processing Technology, 209(4), 1965-1979.
11. Zhang, L., Li L. I., (2013). J. Eng. Mat Sci., 20, 27-34.
12. Xu, R., Zhang, L., Zhu, B., Bu X, I., (2014). J. Eng. Mat Sci., 21, 628-634.
13. Nishida, Y., Droste, W., Engler, S., (1986). Metal. Trans. B, 17B, 833-844.
14. Susac, F., (2011). *Numerical Modeling and Control of the Mold Casting Process – Towards Increased Accuracy of the Aluminum Alloy Cast Parts Through Modeling and Control of the Solidification Process*, Lambert Acad. Publ., Saarbrücken, Germania, ISBN: 978-3-8443-1019-1.
15. Epureanu, A., (2004). *Technological systems. Precision. Stability. Economicity*, Galati University Press, ISBN 973-627-083-1.
16. Susac, F., (2013). The Annals of "Dunărea de Jos" University of Galati, Fascicle V, 61-64.
17. Susac, F., Constantin, I., Banu, M., Epureanu, A., Potecaşu, F., Marin, M., (2011). The Annals of "Dunărea de Jos" University of Galati, Fascile V, 2, 91-94.
18. Lagerstedt, A, (2004). *On the shrinkage of metals and its effect in solidification processing* (PhD thesis), Casting of Metals, Royal Inst. Tech., Stockholm, Sweden.
19. Susac, F., Constantin, I., Banu, M., Epureanu, A., Ohura, K., (2010). The Annals of "Dunărea de Jos" University of Galati, Fascicle V, 65-70.
20. Gangmei, G., Chawang, M., Tamang, S.K., Chandrasekaran, M., (2018). *Fuzzy Set Based Optimization for Grinding Al/SiC MMC; An Approach to Maximize MRR Satisfying Desired Surface Roughness*. International Journal of Modern Manufacturing Technologies, ISSN 2067–3604, X(1), 43-49.
21. Misirli, C., Şahin, M., Ceviz, M., (2017). *The Effects on Surface Roughness of Parameters in Machining*. International Journal of Modern Manufacturing Technologies, ISSN 2067–3604, IX(1), 35-40.

Received: October 02, 2018 / Accepted: June 15, 2019 / Paper available online: June 20, 2019 © International Journal of Modern Manufacturing Technologies.